Ultra-Low Loss Graphene Plasmonic Waveguide for Chip-Scale Terahertz Communication

Lei Sun, Lihao Huang, Yijie Wang, Yu Lian, Guangjing Huang, Huiling Zhao, and Kai Zheng

***Abstract*—Field-programmable photonic array-based chips will be key components in realizing high-performance THz communication in the future. However, the optical diffraction limit prohibits their integration in chip-level sizes. Although plasmonic waveguides combined with graphene are able to possess mode transmission at THz wavelengths, their operational problems such as complex device structures or high transmission losses still cannot be addressed effectively. In this paper, by relying on a mechanism of THz surface plasmon mode of graphene and an energy distribution mechanism of the refractive index difference region, a novel hybrid graphene plasmonic waveguide is proposed, whose core design part is a simple gap-slot region. This waveguide's transmission distance is one order of magnitude longer than that of the conventional waveguide while retaining the benefit high energy confinement, under appropriate parameters. Hence the proposed waveguide can be an efficient candidate component of field-programmable photonic arrays for THz communication.**

***Index Terms*—Graphene, plasmonic waveguide, THz communication.**

I. Introduction

COMPARED to conventional microwave communication systems, the unique advantages of THz systems are the orders-of-magnitude-faster speed and larger transmission bandwidth [1]. However, digital electronic field programmable gate arrays (FPGAs) [2], which are the most important building blocks of electronic integrated circuits, are not able to operate above 1 THz due to the limited cutoff frequency of crystal field effect transistors [3]. Although THz communications can be realized through combinations of complex and bulky free-space optical devices, their large physical dimensions are a bottleneck for chip-level communication systems [4]. Moreover, field programmable photonic arrays (FPPAs) [5] based on cascades of directional photonic couplers allow analog operations such as tunable optical power coupling ratios and phase shifting between input and output photonic waveguides, and can be potentially used for THz communications on a chip level [6], [7]. However, the communication efficiency of FPPAs is seriously inhibited by their low degree of integration due to optical diffraction limit problems in the interior photonic waveguides.

Two-dimensional graphene [8], [9] has metal-like properties in the THz range and allows a graphene plasmon mode that guides THz waves under the physical size beyond the diffraction limit [10], [11]. It can be used in plasmonic waveguides [12]–[19] for THz communication and therefore potentially applied in chip-level communication systems based on highly-integrated FPPAs. However, most graphene plasmonic waveguides [12]–[19] are subject to a trade-off between energy confinement and propagation distance. By leveraging the energy distribution mechanism of materials with large refractive index differences and lossless slot region properties, our previous design for a slot-rib-slot graphene plasmonic waveguide [20] generated hybrid modes that support transmission with sub-wavelength energy confinement. Due to the fact that a large part of the energy converged to a graphene gap region, the previously presented system's transmission loss is higher compared to traditional graphene waveguides. In addition, the key feature of this waveguide is the hybrid slot-rib-slot region which is composed of many complex structures and is therefore difficult to fabricate.

Therefore, in this paper we present a simpler hybrid graphene plasmonic waveguide structure that consists of a high-refractive-index Si cylinder waveguide surrounded by a low-refractive-index SiO_2 background and a grapheme-covered slot filled with low-refractive-index SiO_2 background inside a high-refractive-index Si platform. To the best of our knowledge, this is the first demonstration of a waveguide suitable for ultra-high integration and with ultra-low THz transmission loss. According to the principle of energy convergence in the region of large-difference refractive index and tip structure [21]–[23], a very large amount of electromagnetic energy converges at a sub-wavelength scale

Manuscript received May 24, 2021; revised June 27, 2021; accepted July 12, 2021. Date of publication July 16, 2021; date of current version August 3, 2021. This work was supported in part by the National Natural Science Foundation of China under Grant 62005172, and in part by the Industrial Development and Foster Project of Yangtze River Delta Research Institute of NPU, Taicang under Grant CY20210207. *(Corresponding author: Kai Zheng.)*

Lei Sun is with the Northwestern Polytechnical University, Xi'an City, Shaanxi 710072, China, and also with the Beijing Microelectronics Technology Institute, Beijing City 100076, China (e-mail: sunraygate@126.com).

Lihao Huang is with the China Aerospace Science and Technology Corporation, Beijing City 100094, China (e-mail: 329122929@qq.com).

Yijie Wang is with the Beijing Spacecrafts, Beijing City 100094, China (e-mail: 18801119269@163.com).

Yu Lian is with the China Academy of Space Technology, Beijing City 100094, China (e-mail: 50698150@qq.com).

Guangjing Huang is with the Ju Guang Machinery, Dongguan City, Guangdong 523000, China (e-mail: zongjingli@catocnc.com).

Huiling Zhao is with the Northwestern Polytechnical University, Xi'an City, Shaanxi 710072, China (e-mail: zhhl@nwpu.edu.cn).

Kai Zheng is with the Northwestern Polytechnical University, Xi'an City, Shaanxi 710072, China, and also with the Center for Biomedical Optics and Photonics & College of Physics and Optoelectronic Engineering, Key Laboratory of Optoelectronic Devices and Systems, Shenzhen University, Shenzhen City 518060, China (e-mail: kaizheng@nwpu.edu.cn).

This article has supplementary downloadable material available at https://doi.org/10.1109/JPHOT.2021.3097334, provided by the authors.

Digital Object Identifier 10.1109/JPHOT.2021.3097334

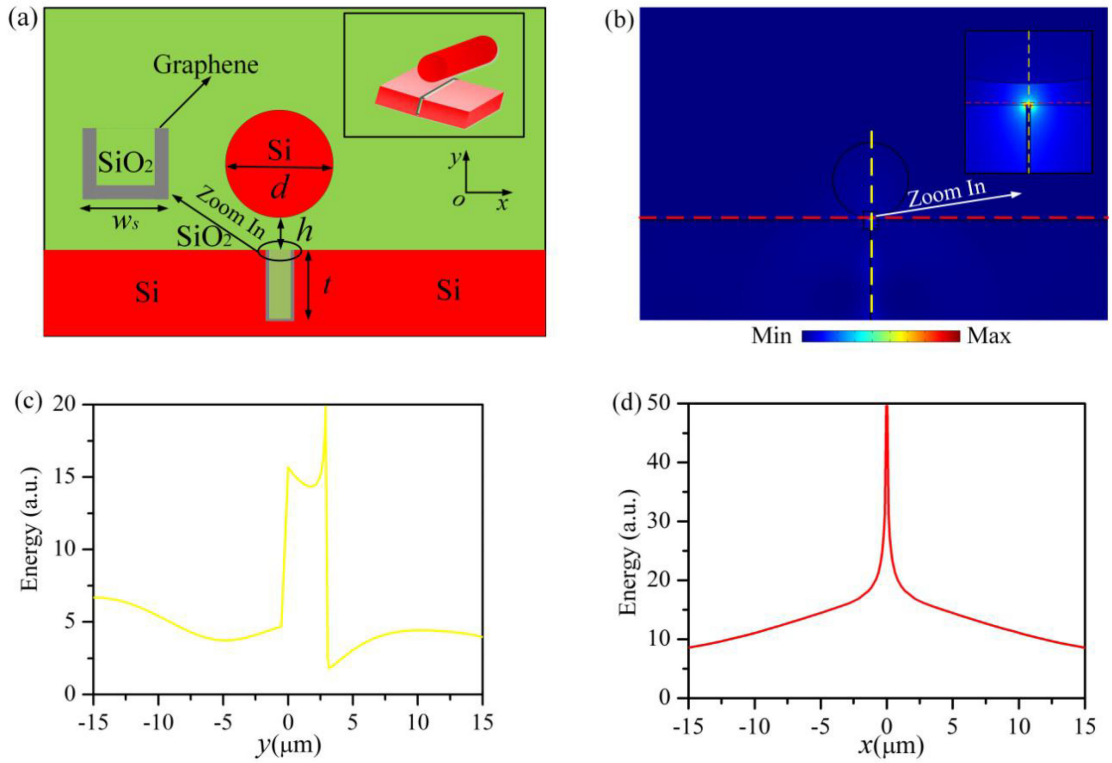

Fig. 1. Structure of the designed waveguide: (a) cross section view (inset: 3D view) and energy distribution of the designed waveguide: (b) modal energy; (c) modal energy at cutline $x = 0$; (d) modal energy at cutline $y = 0$.

near the graphene-slot area, where more energy is concentrated on the lossless slot region rather than graphene region, and hence our proposed system has the potential to form the basis for highly-integrated plasmonic components for THz communications with low power consumption.

II. Structure and Modal Evaluation Indexes

Fig. 1(a) shows the configuration of our designed waveguide, where a Si waveguide with diameter d is placed on a slot region (with width and height of w_s and t, respectively) composed of a graphene layer, an Si substrate and an SiO_2-filled area. A gap region is sandwiched between the Si waveguide and the slot region, where the gap height h is defined as the shortest distance between the Si waveguide and the slot region. In this study, the refractive indices of Si and SiO_2 are assumed to be 3.5 and 1.5, respectively, while the layers and refractive index of the graphene are the same as those of the traditional plasmonic waveguide working at 3 THz frequency [13]. Unlike our previously-designed high energy confinement graphene waveguide [20], whose key structure is a complex hybrid structure including a sharp graphene tip and many areas of different materials, the waveguide proposed in this study is composed of just two types of materials and its core part is a simple graphene-slot region. Therefore, its fabrication process is greatly simplified.

A finite element model built using the Comsol software is used to investigate modal properties of waveguide. In order to understand the energy distribution of the transmission mode, the energy distribution diagram is shown in Fig. 1(b)-(d). It is clear that the most of modal energy is confined at the interface between the gap region and the top surface of the graphene-slot region. This is because our proposed waveguide supports a hybrid transmission mode, which combines the properties of dielectric mode with those of plasmonic mode. The modal energy of the dielectric and plasmonic modes converge more easily at the lower refractive index area within high-difference refractive indices regions and graphene tip region, respectively.

In this paper, three different modal characteristics' indices, namely the normalized mode area, the propagation distance and the figure of merit, are adopted to evaluate the transmission performance of the designed waveguide. The normalized mode area is commonly used to measure energy confinement within a waveguide and can be formulated as [21]:

$$Meff = \frac{Aeff}{A0},\ Aeff = \frac{W_m}{\max(W(r))} = \frac{\iint W(r)d^2r}{\max(W(r))} \tag{1}$$

In (1), A_0 is the diffraction limited mode area in free space, which can be expressed as $\lambda^2/4$, while A_{eff} is the ratio between the total modal energy W_m and the maximum energy density max($W(r)$), whose detailed equation form is shown in [21].

The propagation distance, which is used to measure the transmission loss of waveguides, can be expressed as $L = \lambda/4\pi\mathrm{Im}(Neff)$, where $\mathrm{Im}(Neff)$ is the imaginary part of the guided transmission mode's effective index and λ is the working wavelength. In order to further evaluate the overall performance

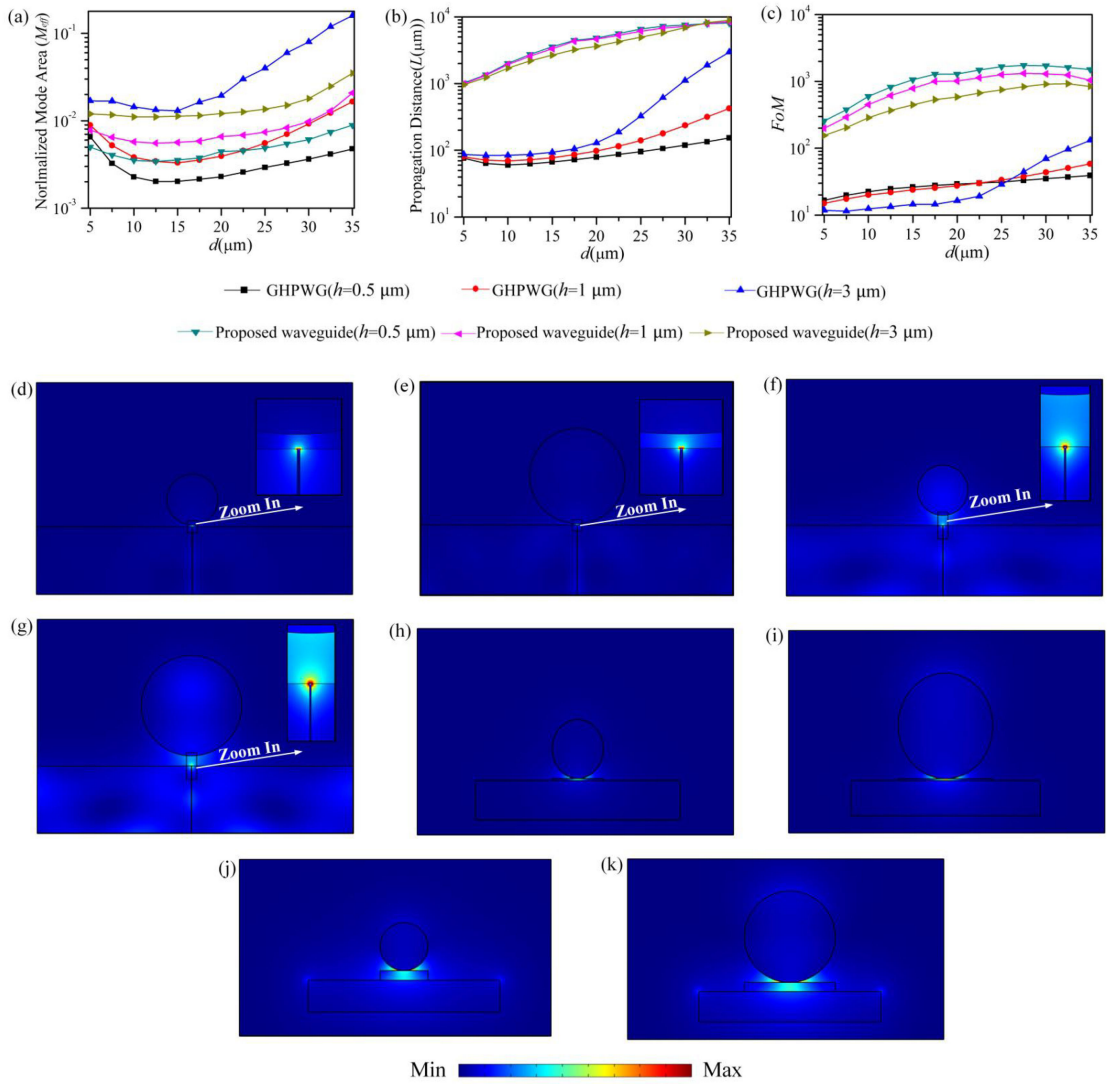

Fig. 2. Dependence of modal properties for the proposed waveguide on d with different h, when setting $w_s = 0.1$ μm and t = 30 μm, as compared with GHPWG (a) normalized mode area; (b) propagation distance; (c) *FoM*; (d)–(g) energy distribution of our designed waveguide with various d and h: (d) [d, h] = [15, 0.5] μm; (e) [d, h] = [30, 0.5] μm; (f) [d, h] = [15], [3] μm; (g) [d, h] = [30, 3] μm; (h)–(k) energy distribution of GHPWG with various d and h: (h) [d, h] = [15, 0.5] μm; (i) [d, h] = [30, 0.5] μm; (j) [d, h] = [15], [3] μm; (k) [d, h] = [30, 3] μm.

of the device's transmission mode, the figure of merit (*FoM*) [24] is employed. Its equation form is $\mathrm{FoM} = L/2\sqrt{M_{eff}/\pi}$.

III. Modal Properties and Discussions

The dependence of the traditional graphene plasmonic waveguide (denoted as GHPWG) and the proposed configuration's modal characteristics on the diameter d of the dielectric waveguide is shown in Fig. 2(a)–(c) for different gap heights h. It is clear that our designed waveguide has an order of magnitude higher propagation distance and the same order of magnitude mode area, both of which result in the figure of merit being one order of magnitude higher compared with the traditional graphene waveguide. This phenomenon can be attributed to the high energy confinement mode converging at the slot region where the material loss is lower than that of graphene, as shown in Fig. 2(d)–(k). Moreover, as d and h increase, more modal energy is concentrated in the gap region, which leads to a higher mode area and propagation distance. In addition, compared with our previously investigated waveguide for THz communication [20], the designed waveguide has a higher FoM and shows lower transmission loss, owing to its ten times longer propagation distance.

Fig. 3 shows the changes of the modal properties as a function of the slot width w_s for various values of d. As evident from Fig. 3(a)–(b), a larger slot region leads to a smaller mode area and propagation distance, which can be explained by the change of the modal properties from long-range plasmonic mode to single-interface plasmonic mode. This is also illustrated in the modal energy distribution variation, shown in Fig. 3(d)–(f). Moreover, a larger mode area and propagation distance is obtained by increasing d, which can be explained by the more dielectric-like modal properties formed. In addition, the behaviors of the *FoM* for different value ranges of d and w_s are completely opposite

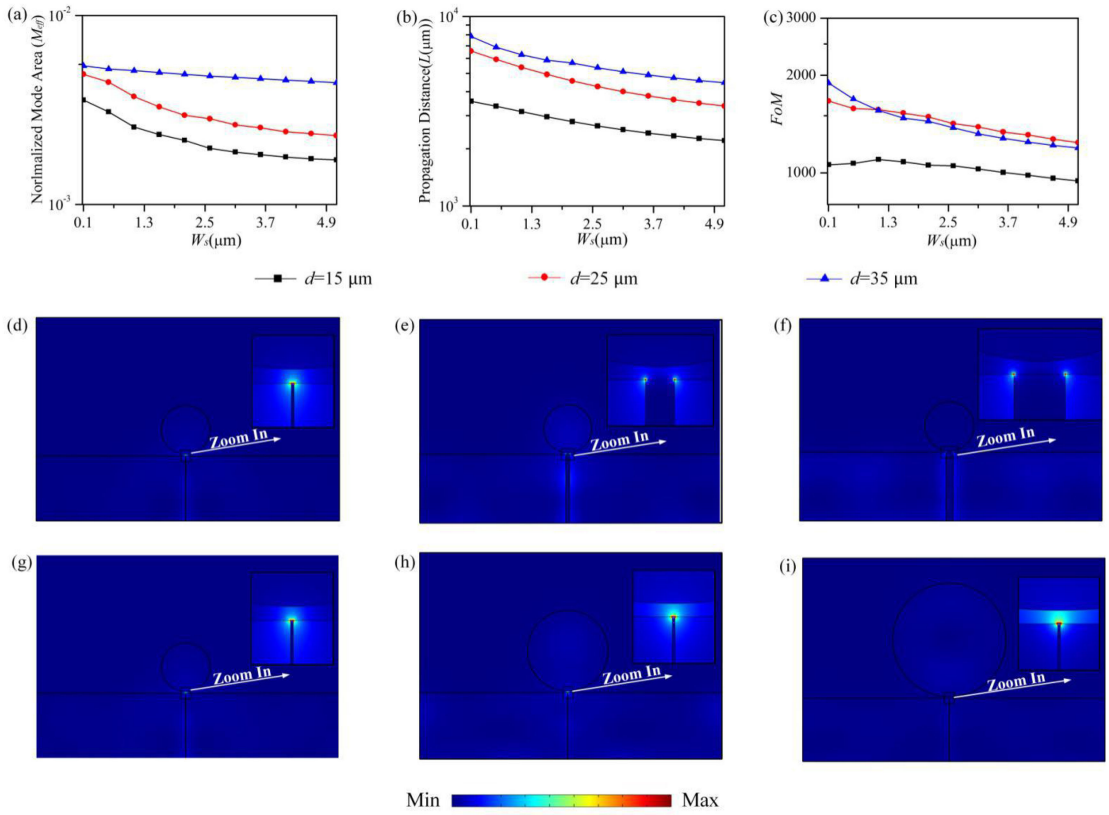

Fig. 3. Dependence of modal properties for the proposed waveguide on w_s with different d, when $t = 30$ μm, and $h = 0.5$ μm: (a) normalized mode area; (b) propagation distance; (c) *FoM*; (d)–(f) energy distribution on *Ws* when $d = 15$ μm: (d) $w_s = 0.1$ μm; (e) $w_s = 1.1$ μm; (f) $w_s = 2.1$ μm; (g)–(i) energy distribution on d when $w_s = 0.1$ μm: (g) $d = 15$ μm; (h) $d = 25$ μm; (i) $d = 35$ μm.

(e.g., ($w_s < 1$ μm vs $w_s > 1$ μm when $d = 15$ μm or $d = 25$ μm) and ($d = 35$ μm vs $d = 25$ μm when w_s changes)), from which is contributed to find the optimum structure size of waveguide.

In order to determine the influence of the slot height t and the tuning effect of the graphene photoelectric properties on the modal properties, the dependence of the modal properties for the proposed waveguide on t for different chemical potentials of graphene V were investigated, as shown in Fig. 4. On one hand, as the slot height t increases, the normalized mode area and propagation distance decrease gradually, and then tend to stabilize after t > 13.5 μm, while there is no apparent change of the *FoM*. This phenomenon can be attributed to the modal energy gradually concentrating from the gap region to a sub-wavelength graphene-slot region, as shown in Figs 4(d)–(f). On the other hand, an increased chemical potential results in a larger real and a smaller imaginary part of the graphene's refractive index, leading to a transmission mode with a decreased energy confinement and propagation loss (illustrated from Fig. 4(g)–(i)), along with a larger propagation distance, mode area and *FoM* (illustrated from Fig. 4(a)–(c)).

To fabricate the proposed waveguide structure, a highly precise Si groove structure can be realized using electron-beam lithography [25], following which a graphene layer can be prepared onto the groove surface through oxidation-reduction [26]. Using plasma-enhanced chemical vapor deposition [27], an insulating SiO_2 layer will be deposited on the Si groove substrate. Then, a highly precise Si cylinder waveguide can be prepared using the nanoparticle-catalyzed vaporliquid-solid method [28].

IV. Crosstalk Discussions

Waveguide crosstalk is one of the most important factors affecting the communication efficiency of chips [29]. Hence, in this paper, modal crosstalk between two parallel waveguides with a center-to-center distance S (shown in Fig. 5(a)) is analyzed through the introduction of the coupling length L_c, defined as $\lambda/2(n_e - n_o)$ in coupled mode theory [30], where n_e and n_o are the effective refractive indices of the symmetric and asymmetric modes, respectively. The influence of the normalized coupling length L_c/L versus the normalized center-to-center distance $(S - d)/d$ for different values of h are investigated, as shown in Fig. 5(b). It is clear that the normalized coupling length is always larger than 1, which indicates that crosstalk is fully suppressed [20]. This can be attributed to the excellent modal energy confinement performance of our designed waveguide. In addition, an effective way to reduce crosstalk is to decrease the gap height h, as seen in Fig. 5(b), due to the resulting increase in modal energy confinement.

V. Summary

In conclusion, a novel modified graphene plasmonic waveguide which consisting of a simple graphene-slot region and

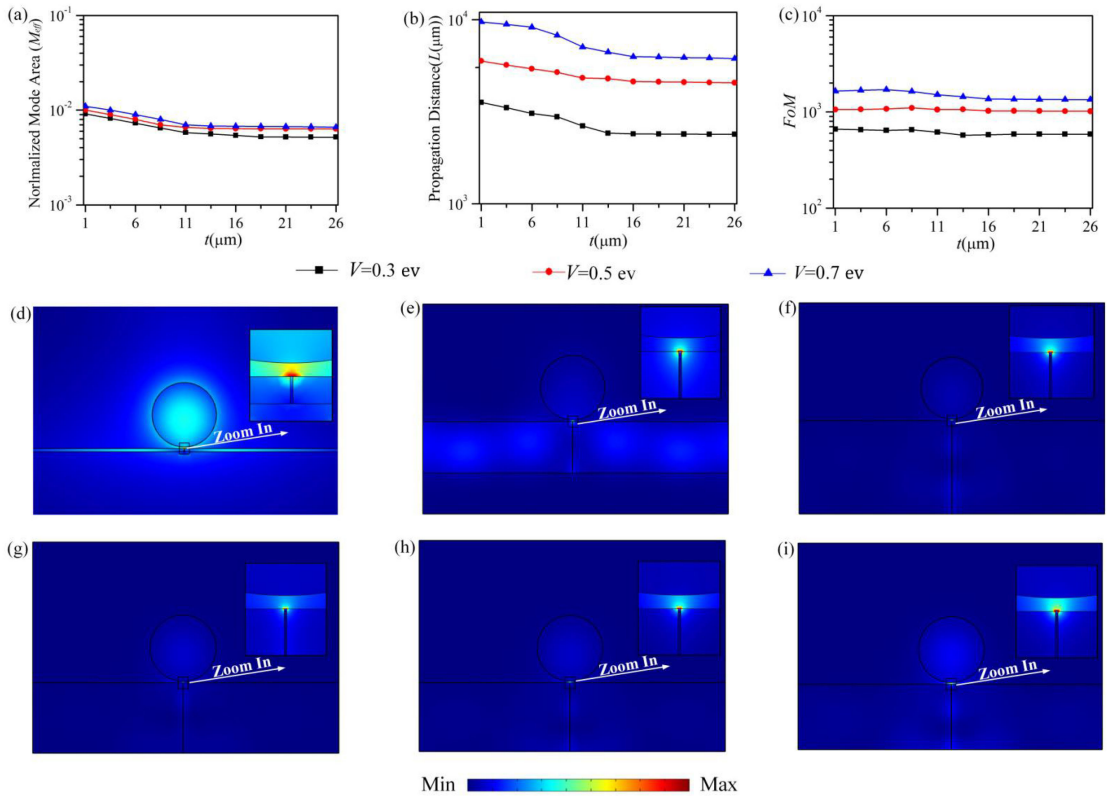

Fig. 4. Dependence of modal properties for the proposed waveguide on t with different V, when $h = 0.5$ μm and $w_s = 0.1$ μm: (a) normalized mode area; (b) propagation distance; (c) *FoM*; (d)–(f) energy distribution on w_s when $V = 0.5$ ev: (d) t $= 1$ μm; (e) t $= 11$ μm; (f) t $= 31$ μm; (g)–(i) energy distribution on V when t $= 31$ μm: (g) $V = 0.3$ ev; (h) $V = 0.5$ ev; (i) $V = 0.7$ ev.

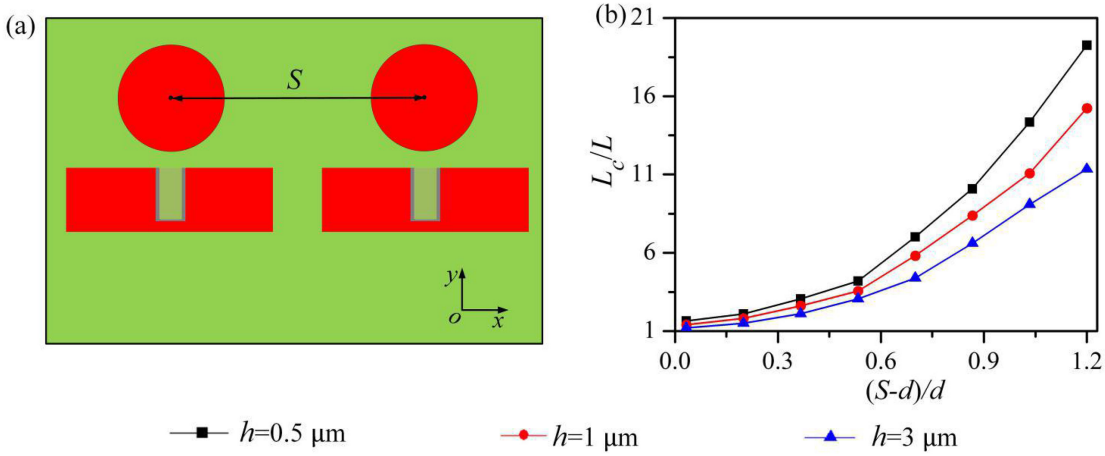

Fig. 5. The crosstalk between two parallel waveguides (a) Geometry of cross section; (b) the influence of the normalized coupling length versus the normalized center-to-center separation distance, with varied h.

a dielectric waveguide is proposed for THz frequency circuit operation. The waveguide can offer a hybrid transmission mode that has at least ten times lower propagation loss and considerable energy confinement compared with its traditional graphene plasmonic waveguide counterparts. The excellent performance of the waveguide makes it an excellent and vital component of FPPAs based on photonic chips for low-loss THz communication. In addition, in order to realize a long-range plasmonic mode which provides a stable energy confinement as well as low-loss transmission, the slot width and the slot height should be adjusted to be smaller than 1 μm and larger than 13 μm, respectively. Furthermore, increasing the chemical potential of graphene will further reduce the transmission loss of the waveguide at the expense of its energy confinement ability. Our designed waveguide shows limited crosstalk for chip communication and paves a new way for ultrahigh-speed signal processing for THz communications.

REFERENCES

[1] T. Kleine-Ostmann and T. Nagatsuma, "A review on terahertz communications research," *J. Infrared, Millimeter, Terahertz Waves*, vol. 32, no. 2, pp. 143–171, 2011.

[2] E. Monmasson E and M. N. Cirstea, "FPGA design methodology for industrial control Systems—A review," *IEEE Trans. Ind. Electron.*, vol. 54, no. 4, pp. 1824–1842, Aug. 2007.

[3] X. Wu, H. Lu, and K. Sengupta, "Programmable terahertz chip-scale sensing interface with direct digital reconfiguration at sub-wavelength scales," *Nature Commun.*, vol. 10, no. 1, pp. 2722-1–2722-13, 2019.

[4] M. Abo-Bakr *et al.*, "Coherent far-infrared (THz) synchrotron radiation," *Phys. Rev. Lett.*, vol. 90, no. 9, pp. 094801-1–094801-4, 2003.

[5] I. G. D.Pérez and J. Capmany, "Field-programmable photonic arrays," *Opt. Exp.*, vol. 26, no. 21, pp. 27265–27278, 2018.

[6] K. Dong *et al.*, "A lithography-free and field-programmable photonic metacanvas," *Adv. Mater.*, vol. 30, no. 5, pp. 1703878-1–1703878-7, 2018.

[7] W. Zhang and J. Yao, "Photonic integrated field-programmable disk array signal processor," *Nature Commun.*, vol. 11, no. 1, pp. 406-1–406-9, 2020.

[8] A. N. Grigorenko, M. Polini, and K. S. Novoselov, "Graphene plasmonics," *Nature Photon.*, vol. 6, no. 11, pp. 749–758, 2012.

[9] A. K. Geim and K. S. Novoselov, "The rise of graphene," *Nature Mater.*, vol. 6, no. 3, pp. 183–191, 2007.

[10] K. M. Daniels *et al.*, "Narrow plasmon resonances enabled by quasi-freestanding bilayer epitaxial grapheme," *2D Mater.*, vol. 4, no. 2, pp. 025034-1–025034-9, 2017.

[11] N. H. Tu, K. Yoshioka, S. Sasaki, M. Takamura, and N. Kumadaet, "Active spatial control of terahertz plasmons in graphene," *Commun. Mater.*, vol. 1, no. 7, pp. 7-1–7-6, 2020.

[12] S. Kumar, S. K. H. Andersen, and S. I. Bozhevolnyi, "Extremely confined gap-plasmon waveguide modes excited by nitrogen-vacancy centers in diamonds," *ACS Photon.*, vol. 6, no. 1, pp. 23–29, 2019.

[13] X. He *et al.*, "Ultralow loss graphene-based hybrid plasmonic waveguide with deep-subwavelength confinement," *Opt. Exp.*, vol. 26, no. 8, pp. 10109–10118, 2018.

[14] J. Guo, J. Li, C. Liu, Y. Yin, and D. Dai, "High-performance silicon-graphene hybrid plasmonic waveguide photodetectors beyond 1.55 μm," *Light: Sci. Appl.*, vol. 9, no. 29, pp. 1–11, 2020.

[15] D. Ansell, I. P. Radko, Z. Han, F. J. Rodriguez, S. I. Bozhevolnyi, and A. N. Grigorenko, "Hybrid graphene plasmonic waveguide modulators," *Nature Commun.*, vol. 6, pp. 8846-1–8846-6, 2015.

[16] Y. Li, K. Tantiwanichapan, A. Swan, and P. Robert, "Graphene plasmonic devices for terahertz optoelectronics," *Nanophotonics*, vol. 9, no. 7, pp. 1901–1920, 2020.

[17] X. Q. He, T. G. Ning, L. Pei, J. J. Zheng, J. Li, and X. D. Wen, "Tunable hybridization of graphene plasmons and dielectric modes for highly confined light transmit at terahertz wavelength," *Opt. Exp.*, vol. 27, no. 5, pp. 961–5972, 2019.

[18] L. Ye, K. Sui, Z. Yong, and Q. H. H. Liu, "Broadband optical waveguide modulators based on strongly coupled hybrid graphene and metal nanoribbons for near-infrared applications," *Nanoscale*, vol. 11, pp. 3229–3239, 2019.

[19] L. Ye, K. Sui, Y. Liu, M. Zhang, and Q. H. Liu, "Graphene-based hybrid plasmonic waveguide for highly efficient broadband mid-infrared propagation and modulation," *Opt. Exp.*, vol. 26, no. 12, pp. 15935–15947, 2018.

[20] K. Zheng *et al.*, "Ultra-compact, low-loss terahertz waveguide based on graphene plasmonic technology," *2D Mater.*, vol. 7, no. 1, pp. 015016-1–015016-8, 2020.

[21] R. F. Oulton, V. J. Sorger, D. A. Genov, D. F. P. Pile, and X. Zhang, "A hybrid plasmonic waveguide for subwavelength confinement and long-range propagation," *Nature Photon.*, vol. 2, no. 8, pp. 496–500, 2008.

[22] K. Zheng *et al.*, "Ultra-high light confinement and ultra-long propagation distance design for integratable optical chips based on plasmonic technology," *Nanoscale*, vol. 11, pp. 4601–4613, 2019.

[23] K. Zheng, J. Song, and J. Qu, "Hybrid low-permittivity slot-rib plasmonic waveguide based on monolayer two dimensional transition metal dichalcogenide with ultra-high energy confinement," *Opt. Exp.*, vol. 26, no no. 12, pp. 15819–15824, 2018.

[24] R. Buckley and P. Berini, "Figures of merit for 2D surface plasmon waveguides and application to metal stripes," *Opt. Exp.*, vol. 15, no. 19, pp. 12174–12182, 2007.

[25] M. Gully-Santiago, D. T. Jaffe, C. B. Brooks, D. W. Wilson, and R. E. Muller, "High performance Si immersion gratings patterned with electron beam lithography," in *Proc. SPIE 9151, Adv. Opt. Mech. Technol. for Telescopes Instrum.*, 2014, pp. 91515K-1–91515K-13.

[26] V. H. Pham *et al.*, "Fast and simple fabrication of a large transparent chemically-converted graphene film by spray-coating," *Carbon*, vol. 48, no. 7, pp. 1945–1951, 2010.

[27] K. H. A. Bogart, N. F. Dalleska, G. R. Bogart, and R. Ellen, "FisherPlasma enhanced chemical vapor deposition of SiO_2 using novel alkoxysilane precursors," *J. Vac. Sci. Technol. A: Vac., Surfaces, Films*, vol. 13, no. 2, pp. 476–480, 1995.

[28] F. Patolsky, G. Zheng, and C. M. Lieber, "Fabrication of silicon nanowire devices for ultrasensitive, label-free, real-time detection of biological and chemical species," *Nature Protoc.*, vol. 1, no. 4, pp. 1711–1724, 2006.

[29] Y. Fang and M. Sun, "Nanoplasmonic waveguides: Towards applications in integrated nanophotonic circuits," *Light Sci. Appl.*, vol. 4, no. 6, pp. e294-1–e294-11, 2015.

[30] V. Georgios and S. Fan, "Crosstalk between three-dimensional plasmonic slot waveguides," *Opt. Exp.*, vol. 16, no. 3, pp. 2129–2129, 2008.